LETTERS

A bacterial dynamin-like protein

Harry H. Low[1] & Jan Löwe[1]

Dynamins form a superfamily of large mechano-chemical GTPases that includes the classical dynamins and dynamin-like proteins (DLPs)[1]. They are found throughout the Eukarya, functioning in core cellular processes such as endocytosis and organelle division[1]. Many bacteria are predicted by sequence to possess large GTPases with the same multidomain architecture that is found in DLPs[2]. Mechanistic dissection of dynamin family members has been impeded by a lack of high-resolution structural data currently restricted to the GTPase[3,4] and pleckstrin homology[5] domains, and the dynamin-related human guanylate-binding protein[6]. Here we present the crystal structure of a cyanobacterial DLP in both nucleotide-free and GDP-associated conformation. The bacterial DLP shows dynamin-like qualities, such as helical self-assembly and tubulation of a lipid bilayer. *In vivo*, it localizes to the membrane in a manner reminiscent of FZL[7], a chloroplast-specific dynamin-related protein with which it shares sequence similarity. Our results provide structural and mechanistic insight that may be relevant across the dynamin superfamily. Concurrently, we show compelling similarity between a cyanobacterial and chloroplast DLP that, given the endosymbiotic ancestry of chloroplasts[8], questions the evolutionary origins of dynamins.

Dynamins are distinguished from classical signalling GTPases by their large size (~100 kDa)[9], low affinity for GTP[10], high basal GTP hydrolysis rate[10], and self-assembly into filamentous rings[11] and helices[12]. Minimally, all family members have a GTPase domain, middle domain and GTPase effector domain (GED)[1]. GTPase activity is cooperative, with the basal rate increasing between 10- and 100-fold under conditions that promote self-assembly into oligomers[13–15]. Dynamins promote the fission or fusion of membrane by binding to lipid through the pleckstrin homology (PH) domain in classical dynamins[16] or through a functionally equivalent yet non-conserved region in DLPs located between the middle domain and GED[1]. *In vitro*, helical dynamin filaments tubulate liposomes[17,18] and coat preformed lipid tubes[13].

Many Eubacteria have hypothetical genes that tentatively encode dynamin-like proteins containing a GTPase domain, middle domain and GED[2]. Such proteins include ZP_00108538 (Genbank accession code) from the filamentous cyanobacterium *Nostoc punctiforme*, which is the subject of this study and which we term bacterial dynamin-like protein (BDLP). Purified *N. punctiforme* BDLP is a GTPase with a Michaelis constant (K_m) of 68.6 μM and a catalytic rate constant (k_{cat}) of 0.53 min^{-1} (Fig. 1a, b), which is in the range of the dynamin family[1,19]. The P-loop mutant K82A reduces GTPase activity about 15-fold (Fig. 1b). Western blot analysis against *N. punctiforme* whole-cell lysate shows that this protein is produced *in vivo* (Fig. 1c).

In the presence of GMPPNP (a non-hydrolysable GTP analogue) and either *N. punctiforme* (not shown) or *Escherichia coli* whole-cell lipid extract extruded to form liposomes, BDLP strikingly self-assembles, binding to the lipid bilayer in a regular pattern (Fig. 1d–f and Supplementary Fig. 1g, h). Liposomes are tubulated in a compact helical coating with a 60 Å interfilament pitch repeat and a diameter of ~45 nm. Broken coated tube stubs yield a detailed cross-sectional view into the helix, which appears as a cartwheel with 17-fold rotational symmetry (Fig. 1e, f). Thin radial spokes of ~80 Å merge

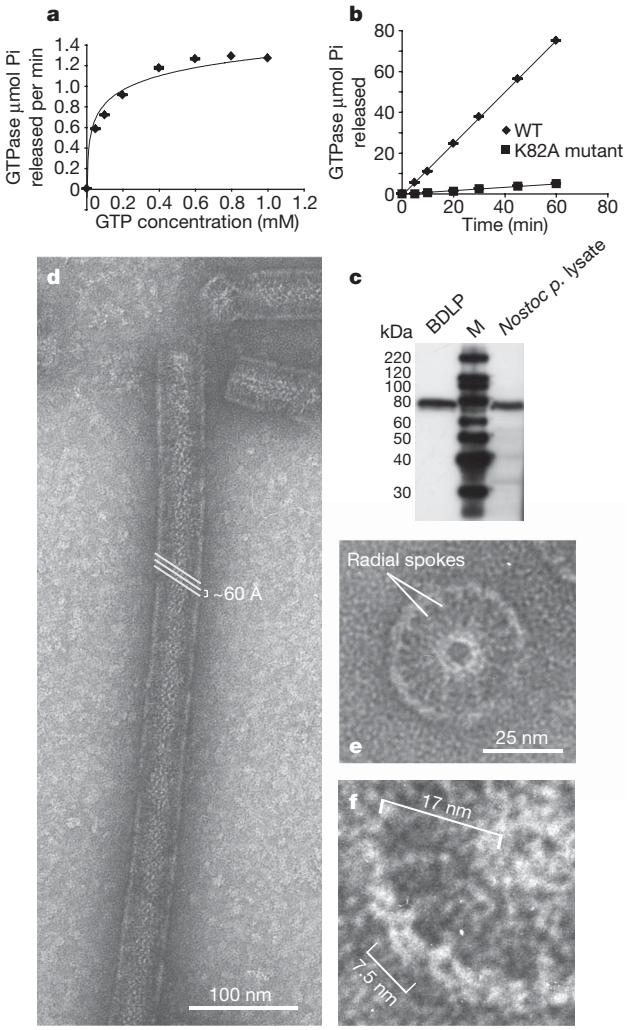

Figure 1 | BDLP is a GTPase capable of decorating and tubulating liposomes. a, Basal GTP hydrolysis rates for 2.5 μM BDLP (ZP_00108538 from *N. punctiforme*) at variable GTP concentration. **b**, Time course comparing GTP hydrolysis of wild-type (WT) and K82A (Walker A) mutant BDLP. Error bars represent the s.d. from three independent experiments. **c**, Western blot analysis. Left, BDLP purifies as a single band at 79.4 kDa (including the C-terminal 6×His tag and N-terminal Gly-Ser-His linker). Right, BDLP is expressed in vegetatively growing *N. punctiforme*. **d**, In the presence of 2 mM GMPPNP, BDLP (25 μM) decorates and tubulates *E. coli* lipid liposomes. A 60 Å interfilament pitch repeat is deduced from diffraction analysis (not shown). **e**, **f**, Decorated tube stubs in cross-section reveal the internal organization of the helix.

[1]MRC Laboratory of Molecular Biology, Hills Road, Cambridge CB2 2QH, UK.

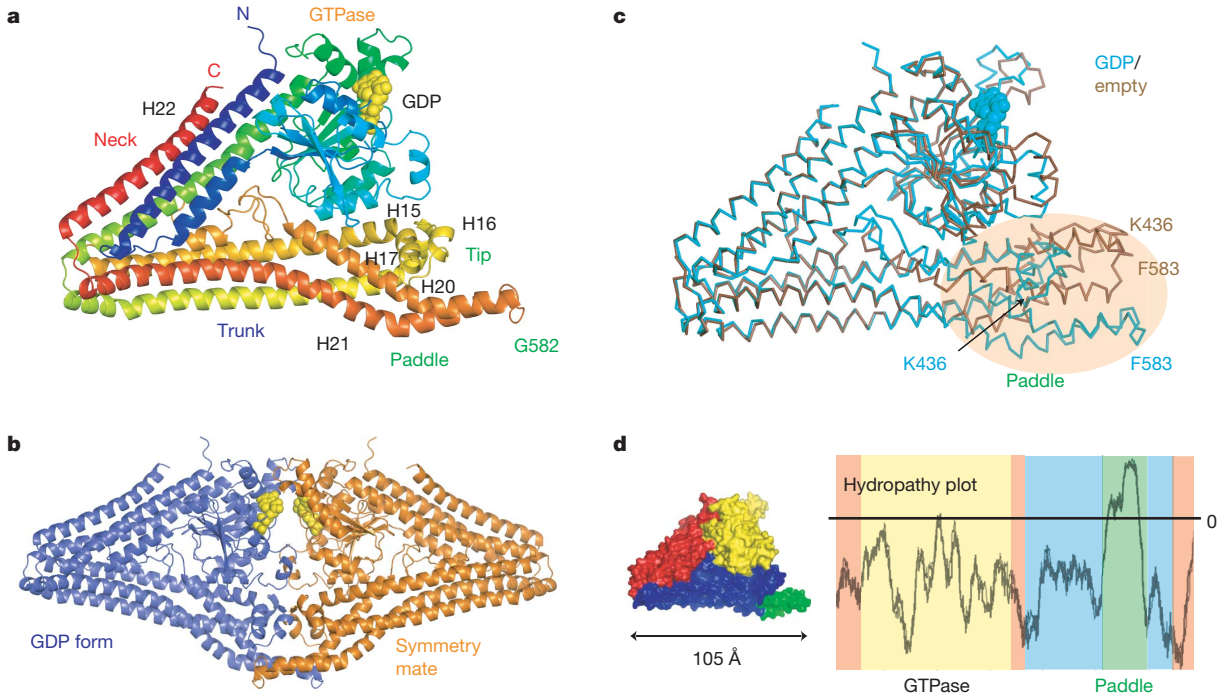

Figure 2 | Crystal structures of BDLP in GDP-associated and nucleotide-free conformations. **a**, The BDLP-GDP monomer and domain assignment. The monomer is rainbow-coloured from the N (blue) to the C (red) terminus. **b**, GDP binding promotes homodimerization, which buries the GTPase domain nucleotide-binding sites and induces tip interplay. **c**, Main chain superposition showing structural reorganization between the GDP-bound and nucleotide-free states. Note the significant conformational change at the tip. **d**, Surface plot of the GDP monomer coloured by core regions: yellow, GTPase domain; red, neck region; blue, trunk region; green, paddle region (left). Similarly colour-coded hydropathy plot (TMpred) strongly predicts that the paddle region (residues 572–606) is transmembrane (right).

into a dense outer ring forming a T-shape repeat, while presumably associating with the lipid tube on the inside. Such architecture is reminiscent of eukaryotic dynamin liposome tubulation[18] and three-dimensional (3D) electron microscopy dynamin tube[20,21] and ring[22] reconstructions, which have approximate 14- and 11-fold radial symmetry, respectively. All reconstructions seem to show that the basic assembly unit is a T-shaped repeat, which is thought to comprise a dimer. Further characterization of BDLP in the presence or absence of *E. coli* lipid liposomes and different nucleotides is given in Supplementary Fig. 1 and Supplementary Information.

We did not detect any increase in GTPase activity stimulated by *N. punctiforme* or *E. coli* whole-cell lipid extract. This was unexpected given the striking lipid-induced self-assembly observed by electron microscopy. Activation may require highly specific membrane organization or other unknown cellular binding partners.

We crystallized *N. punctiforme* BDLP in a GDP-associated and a nucleotide-free state. The structures were solved to a resolution of 3.1 Å and 3.0 Å, respectively (Table 1 and Supplementary Table 1). In either form, the molecule is surprisingly compact given the electron microscopy data, and comprises a GTPase head, a four-helix neck and trunk bundle, and a tip domain (Fig. 2a and Supplementary Fig. 2e). On the basis of sequence alignments, DLPs have traditionally been divided into conserved domains consisting of the GTPase domain, middle domain and GED; in BDLP, however, the predicted middle domain and GED do not form discrete entities and instead run in parallel, as four helix bundles, contributing to both the neck and trunk regions. The GTPase domain (residues 68–287) has a long helix–loop–helix amino terminus (1–67), which substantially buttresses the neck. The predicted GED domain at the carboxy terminus of the molecule (607–693) does not make contact with the GTPase domain and is probably involved only in oligomerization. The tip region seems highly specialized and comprises two helical layers (Fig. 2a). Helices 15, 16 and 17 (412–449), derived from the predicted middle domain, form a flexible upper layer, whereas the C terminus of helix 20 linked to the N terminus of helix 21 (572–606) forms a mobile paddle at the base of the molecule. This paddle is positioned between the predicted middle domain and GED and would be expected to mediate lipid binding. Remarkably, given the high solubility of BDLP without detergent, both paddle helices are strongly predicted to be transmembrane (Fig. 2d). Insertion of the paddle into the lipid bilayer could be used as a mechanism to promote membrane curvature. In classical eukaryotic dynamin, the additional PH domain may either replace the paddle region or act in concert by adding lipid binding specificity.

Table 1 | Refinement statistics

	Empty	GDP
Model	4 monomers per asymmetric unit; chains A–D; residues 4–501, 510–526, 540–695; 0 nucleotide; 0 water	1 monomer per asymmetric unit; chain A, residues 2–97, 103–501, 511–695; 1 GDP, 0 Mg^{2+}; 0 water
Diffraction data	3.0 Å, all data	3.1 Å, all data
R factor, R_{free}	0.24 (0.34), 0.28 (0.39)	0.22 (0.35), 0.27 (0.36)
B factors	65.1 $Å^2$, 0.5 $Å^2$	69.3 $Å^2$, 3.3 $Å^2$
Geometry	0.009 Å, 1.226°	0.007 Å, 1.259°
Restrained NCS	0.12 Å	NA
Protein Data Bank accession code	2J69	2J68

B factors, average and root-mean-square deviation between bonded atoms; geometry, root-mean-square deviation for bond lengths and angles from ideal values; NA, not applicable. *R* factor and R_{free} high-resolution bin values shown in parentheses.

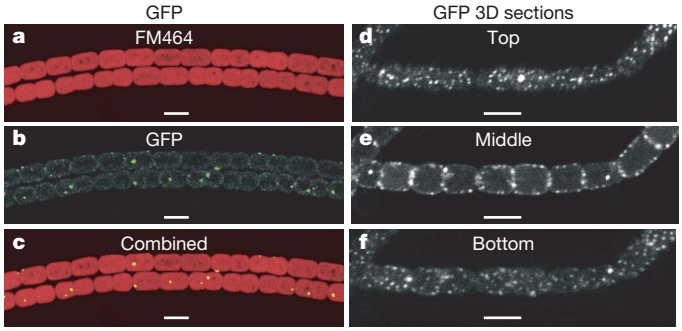

Figure 3 | BDLP shows a punctate pattern of localization in filamentous *N. punctiforme*. Scale bars, 4 μm. **a**–**c**, BDLP–GFP fusion forms a low number of foci at the cell periphery. **d**–**f**, BDLP–GFP punctate localization is restricted to the cell envelope. Shown are 0.2 μm sections taken through the top, middle and bottom of the cell filament.

Binding of GDP promotes formation of a crystallographic dimer with a substantial interface of 7.3% of the monomer surface (2,327/32,044 Å; Fig. 2b). Homodimerization occurs between GTPase domains and occludes the nucleotide-binding site. Helix 9 reaches across the interface and Glu 245 located at the C-terminal tip of the helix is in a position to hydrogen bond with and to stabilize the *trans* nucleotide base (Supplementary Fig. 2f). Significantly, similar GTPase homodimerization across the nucleotide-binding site has been observed in the structure of the GTPase domain of another dynamin family member, human guanylate-binding protein[23] (Supplementary Fig. 2i), and may emerge to be a basic feature of the dynamin family. Homodimerization in human guanylate-binding protein generates a conformation in which Arg 48 located in the P-loop is oriented in *cis* for efficient nucleotide catalysis. Lys 79 in BDLP is found at the equivalent location and could serve a similar purpose (Supplementary Fig. 2g). Tip helices 15, 16 and 17 are heavily kinked, running almost perpendicular to the trunk axis, and are intimately interleaved with the upper paddle surface of the symmetry mate (Fig. 2b). Analytical ultracentrifugation (AUC) of BDLP in the presence of GDP shows a monomer–dimer equilibrium with a dissociation constant (K_d) of 30 μM (Supplementary Fig. 2j). The nucleotide-free monomer forms a non-crystallographic dimer also across the GTPase active site, but with a limited interface of 3.3% of the monomer surface (1,019/31,339 Å). AUC data of BDLP in the absence of nucleotide is shown in Supplementary Fig. 2j.

Nucleotide release promotes rearrangement of the active site with Asp 98 projecting into and occluding the P-loop (Supplementary Fig. 2h). Conserved Thr 103 in the switch 1 region, which is critical for catalysis in GTPases, is orientated away from the active site. The most significant conformational change occurs, however, in the tip. Helices 15, 16 and 17 release the symmetry mate paddle and straighten, realign with the trunk axis, and occlude the upper surface of their own paddle, which has swung up to make contact, thereby providing a potential mechanism to shear the GDP dimer apart (Fig. 2c). Phe 583 located at the paddle tip moves up 21 Å, whereas Lys 436 between helices 16 and 17 traverses 25 Å.

The GDP dimer forms a compact diamond-shaped unit with a maximal distance of 80 Å from the base of the paddles to the top of the GTPase domains (Fig. 2b). In this conformation, BDLP is probably unable to generate the T-shaped repeats that are observed in decorated lipid tube cross-sections in the presence of GMPPNP (Fig. 1e, f). This difference is suggestive of a substantial intramolecular rearrangement in which the region between neck and trunk acts as a hinge that opens and markedly extends the molecule on GTP or lipid binding. In such a conformation, homodimerization across the GTPase domain interface would be expected, as observed in the GDP-associated BDLP crystal structure.

In vivo localization data were obtained by transforming wild-type *N. punctiforme* with a plasmid-borne translational fusion of BDLP and green fluorescent protein (GFP) driven by the wild-type promoter. Using confocal fluorescence microscopy, we observed foci localizing clearly to the cell periphery (Fig. 3a–f). The quantity of foci varied considerably, probably owing to differences in expression, ranging from just a few foci per cell (Fig. 3a–c) to an even covering of foci throughout the cell envelope (Fig. 3d–f). Preferential localization of the GFP fusion was sometimes observed at the cell septum (Supplementary Fig. 3g, h, inset) and ring-like structures could be seen (Supplementary Fig. 3h), although such phenomena were observed only rarely. Immunofluorescence microscopy using an affinity purified antibody raised against BDLP showed a similar localization pattern to the GFP fusion (Supplementary Fig. 3i–k). Foci predominantly localized to the cell membrane, although, in contrast to the GFP fusion, punctate localization was also observed in the cell interior.

Sequence alignments of BDLP with other dynamin family members show that BDLP is most closely related to the mitofusin class of DLPs, which includes *Drosophila* mitochondrial Fzo homologues[24–27] and *Arabidopsis* chloroplast FZL[7] (Supplementary Fig. 3l). The mitofusins have a predicted domain architecture similar to BDLP, including two transmembrane regions at the C terminus that are separated by a short linker and flanked by predicted coiled-coil domains. Alignment of BDLP and FZL (initiated at the P-loop owing to a FZL N-terminal chloroplast import sequence) appears superior to other dynamin family members, with 22% identity and 37% similarity. FZL–GFP in *Arabidopsis* chloroplasts shows a punctate localization pattern at both the chloroplast inner-envelope membrane and topologically bordering thylakoid membranes[7]. BDLP–GFP and immunofluorescence microscopy studies show a strikingly similar punctate phenotype. Given the endosymbiotic origins of chloroplasts from a cyanobacteria, the crystal structure of BDLP may represent FZL and possibly the mitofusin class of DLPs. *fzl* knockout mutants have altered chloroplast morphology, plant growth and thylakoid ultrastructure[7], which can be rescued by FZL–GFP. BDLP may therefore have a similar role in the cyanobacterium *N. punctiforme* in determining thylakoid morphology and cell shape.

Given the presence of large GTPases with predicted dynamin-like domain organization in many members of the Eubacteria such as *E. coli* and *Bacillus subtilis*, it is likely that bacterial dynamins, or BDLPs as we term this class, are not restricted to cyanobacteria. Such observation, combined with our results, suggests a bacterial ancestry for the dynamin superfamily.

METHODS

Cloning, expression and purification. The coding sequence for BDLP from *N. punctiforme* (ZP_00108538) was cloned with a N-terminal MBP fusion, TEV cleavage site in the linker, and His tag at the C terminus. The protein was expressed in *E. coli* strain BL21(DE3). The BDLP–MBP fusion was purified with nickel-Sepharose. MBP was cleaved from BDLP and separated by gel filtration. Purified BDLP includes an additional Gly-Ser-His sequence at the N terminus and a 6×His at the C terminus (see Supplementary Methods for more details).

Crystallization, structure determination and refinement. Initial BDLP crystallization conditions were found in a screen of 1,500 conditions set up by a high-throughput nanolitre robotic system[28]. Native and seleno-methionine BDLP was crystallized by vapour diffusion. BDLP in the nucleotide-free state was initially solved by seleno-methionine multiwavelength anomalous diffraction, whereas BDLP-GDP was solved by molecular replacement (see Supplementary Methods for more details).

Electron microscopy and GTPase assays. *E. coli* whole-cell lipid extract was used to make liposomes. For tubulation, 2 mM GMPPNP was incubated at 37 °C with 25 μM BDLP and 2 mg ml^{-1} of liposomes. Grids were negatively stained. GTPase assays were done with a malachite-green-based kit (see Supplementary Methods for more details).

For details of western blotting, immunofluorescence microscopy, construction of BDLP–GFP reporter and GFP studies, cell culture and phylogenetic analysis, see Supplementary Methods.

Received 13 July; accepted 2 October 2006.
Published online 22 November 2006.

1. Praefcke, G. J. & McMahon, H. T. The dynamin superfamily: universal membrane tubulation and fission molecules? *Nature Rev. Mol. Cell Biol.* **5,** 133–147 (2004).
2. van der Bliek, A. M. Functional diversity in the dynamin family. *Trends Cell Biol.* **9,** 96–102 (1999).
3. Reubold, T. F. *et al.* Crystal structure of the GTPase domain of rat dynamin 1. *Proc. Natl Acad. Sci. USA* **102,** 13093–13098 (2005).
4. Niemann, H. H., Knetsch, M. L., Scherer, A., Manstein, D. J. & Kull, F. J. Crystal structure of a dynamin GTPase domain in both nucleotide-free and GDP-bound forms. *EMBO J.* **20,** 5813–5821 (2001).
5. Ferguson, K. M., Lemmon, M. A., Schlessinger, J. & Sigler, P. B. Crystal structure at 2.2 Å resolution of the pleckstrin homology domain from human dynamin. *Cell* **79,** 199–209 (1994).
6. Prakash, B., Praefcke, G. J., Renault, L., Wittinghofer, A. & Herrmann, C. Structure of human guanylate-binding protein 1 representing a unique class of GTP-binding proteins. *Nature* **403,** 567–571 (2000).
7. Gao, H., Sage, T. L. & Osteryoung, K. W. FZL, an FZO-like protein in plants, is a determinant of thylakoid and chloroplast morphology. *Proc. Natl Acad. Sci. USA* **103,** 6759–6764 (2006).
8. McFadden, G. I. Endosymbiosis and evolution of the plant cell. *Curr. Opin. Plant Biol.* **2,** 513–519 (1999).
9. Obar, R. A., Collins, C. A., Hammarback, J. A., Shpetner, H. S. & Vallee, R. B. Molecular cloning of the microtubule-associated mechanochemical enzyme dynamin reveals homology with a new family of GTP-binding proteins. *Nature* **347,** 256–261 (1990).
10. Song, B. D. & Schmid, S. L. A molecular motor or a regulator? Dynamin's in a class of its own. *Biochemistry* **42,** 1369–1376 (2003).
11. Hinshaw, J. E. & Schmid, S. L. Dynamin self-assembles into rings suggesting a mechanism for coated vesicle budding. *Nature* **374,** 190–192 (1995).
12. Carr, J. F. & Hinshaw, J. E. Dynamin assembles into spirals under physiological salt conditions upon the addition of GDP and γ-phosphate analogues. *J. Biol. Chem.* **272,** 28030–28035 (1997).
13. Stowell, M. H., Marks, B., Wigge, P. & McMahon, H. T. Nucleotide-dependent conformational changes in dynamin: evidence for a mechanochemical molecular spring. *Nature Cell Biol.* **1,** 27–32 (1999).
14. Warnock, D. E., Hinshaw, J. E. & Schmid, S. L. Dynamin self-assembly stimulates its GTPase activity. *J. Biol. Chem.* **271,** 22310–22314 (1996).
15. Tuma, P. L. & Collins, C. A. Activation of dynamin GTPase is a result of positive cooperativity. *J. Biol. Chem.* **269,** 30842–30847 (1994).
16. Salim, K. *et al.* Distinct specificity in the recognition of phosphoinositides by the pleckstrin homology domains of dynamin and Bruton's tyrosine kinase. *EMBO J.* **15,** 6241–6250 (1996).
17. Danino, D., Moon, K. H. & Hinshaw, J. E. Rapid constriction of lipid bilayers by the mechanochemical enzyme dynamin. *J. Struct. Biol.* **147,** 259–267 (2004).
18. Sweitzer, S. M. & Hinshaw, J. E. Dynamin undergoes a GTP-dependent conformational change causing vesiculation. *Cell* **93,** 1021–1029 (1998).
19. Narayanan, R., Leonard, M., Song, B. D., Schmid, S. L. & Ramaswami, M. An internal GAP domain negatively regulates presynaptic dynamin *in vivo*: a two-step model for dynamin function. *J. Cell Biol.* **169,** 117–126 (2005).
20. Zhang, P. & Hinshaw, J. E. Three-dimensional reconstruction of dynamin in the constricted state. *Nature Cell Biol.* **3,** 922–926 (2001).
21. Chen, Y. J., Zhang, P., Egelman, E. H. & Hinshaw, J. E. The stalk region of dynamin drives the constriction of dynamin tubes. *Nature Struct. Mol. Biol.* **11,** 574–575 (2004).
22. Klockow, B. *et al.* The dynamin A ring complex: molecular organization and nucleotide-dependent conformational changes. *EMBO J.* **21,** 240–250 (2002).
23. Ghosh, A., Praefcke, G. J., Renault, L., Wittinghofer, A. & Herrmann, C. How guanylate-binding proteins achieve assembly-stimulated processive cleavage of GTP to GMP. *Nature* **440,** 101–104 (2006).
24. Hales, K. G. & Fuller, M. T. Developmentally regulated mitochondrial fusion mediated by a conserved, novel, predicted GTPase. *Cell* **90,** 121–129 (1997).
25. Hermann, G. J. *et al.* Mitochondrial fusion in yeast requires the transmembrane GTPase Fzo1p. *J. Cell Biol.* **143,** 359–373 (1998).
26. Santel, A. & Fuller, M. T. Control of mitochondrial morphology by a human mitofusin. *J. Cell Sci.* **114,** 867–874 (2001).
27. Rapaport, D., Brunner, M., Neupert, W. & Westermann, B. Fzo1p is a mitochondrial outer membrane protein essential for the biogenesis of functional mitochondria in *Saccharomyces cerevisiae*. *J. Biol. Chem.* **273,** 20150–20155 (1998).
28. Stock, D., Perisic, O. & Löwe, J. Robotic nanolitre protein crystallisation at the MRC Laboratory of Molecular Biology. *Prog. Biophys. Mol. Biol.* **88,** 311–327 (2005).

Supplementary Information is linked to the online version of the paper at www.nature.com/nature.

Acknowledgements We acknowledge support on beamlines ID29, ID14eh4 and ID23eh1 at the ESRF. We thank J. Meeks and K. Hagan for supplying bacterial strains and *N. punctiforme* plasmids including pSCR202; S. Reichelt for support with confocal microscopy; and J. Butler for performing the analytical ultracentrifugation experiments. We thank the MRC for a PhD student fellowship to H.H.L.

Author Information Atomic coordinates produced in this study have been deposited in the Protein Data Bank under accession codes 2J69 (BDLP) and 2J68 (BDLP-GDP). Reprints and permissions information is available at www.nature.com/reprints. The authors declare no competing financial interests. Correspondence and requests for materials should be addressed to J.L. (jyl@mrc-lmb.cam.ac.uk).